Fracture Analysis of Particulate MEE Materials Using a Domain-Independent Interaction Integral Method

Hongjun Yu[1,3,*], **Linzhi Wu**[2,*]

[1] Institute of Applied Mathematics, Harbin Institute of Technology, Harbin 150001, China
[2] Center for Composite Materials, Harbin Institute of Technology, Harbin 150001, China
[3] School of Civil Engineering, Harbin Institute of Technology, Harbin 150001, China
* Corresponding author: yuhongjun@hit.edu.cn (Hongjun Yu); wlz@hit.edu.cn (Linzhi Wu)

Abstract This paper first introduces an expanded tensor notation to express the basic relations of magneto-electro-elastic (MEE) media and then, derives a domain formulation of the interaction integral on the basis of the expanded tensor notation for computing the intensity factors (IFs). The present interaction integral does not require material properties to be differentiable and moreover, it is domain-independent for material interfaces, which may make the interaction integral to become one of the most promising techniques in analyzing the crack problems of MEE composites. Then, the numerical implementation of the interaction integral combined with the extended finite element method (XFEM) is introduced. Using this method, the crack problems of a particulate MEE plate are studied.

Keywords Magneto-electro-elastic (MEE), Crack, Interaction integral, Intensity factors (IFs), Extended finite element method (XFEM)

1. Introduction

Magneto-electro-elastic (MEE) materials have drawn significant interest in several engineering fields as a class of important functional materials, such as magnetic field probes, electronic packaging, actuators, waveguides, sensors, phase investors, transducers. However, a great drawback of MEE materials is their inherent brittleness and low fracture toughness. Generally, these materials may fail prematurely in service due to some defects arising during the manufacturing process and thus, it is of practical significance to learn the fracture feature of MEE materials. Liu et al. [1] studied Green's functions for a cracked MEE body. Wang and Mai [2] obtained a general two-dimensional (2D) solution of the MEE fields around the crack tip. Gao et al. [3] derived an explicit solution in closed form for the intensity factors (IFs) and electro-magnetic fields inside a crack in MEE media. After that, considerable theoretical research works were carried out on the fracture problems of MEE materials. However, most of the theoretical research works restrict MEE media to be infinite and only a few simple configurations can be solved. Therefore, numerical techniques are usually employed in actual fracture analyses of MEE materials.

Among numerical methods, the interaction integral has generated a great interest for its convenience in decoupling mechanical stress intensity factors (SIFs), electric displacement intensity factor (EDIF) and magnetic induction intensity factor (MIIF). The interaction integral was proposed by Stern et al. [4] to decouple mechanical mode-I and mode-II SIFs on the basis of the J-integral by a superposition of two admissible states. Recently, the interaction integral was extended to solve the IFs of piezoelectric (PE) media [5] and those of MEE media [6]. For MEE materials, the interaction integral published previously has a shortcoming that is it requires the material properties to be differentiable. Generally, MEE materials are a category of composites composed of PE and PM phases, and the interfaces between constituent phases may reduce their reliability since the interfaces generally act as sources of failures in service. Therefore, the interfaces can not be ignored when the fracture behaviors of MEE composites are concerned. Fortunately, Yu et al. [7] have developed a new interaction integral for PE solids which is domain-independent for material interfaces. This point brings a great convenience to the fracture analysis of the composites with

complex interfaces. Then, this paper will derive a domain-independent interaction integral for MEE composites.

2. Basic relations and interaction integral

2.1. Basic equations for PE media

The field equations for a linear MEE medium in the absence of body forces, volume charge and concentrated magnetic source are given as follows.

2.1.1. Governing equations

- Constitutive equations

$$\begin{aligned} \sigma_{ij} &= C_{ijkl}\varepsilon_{kl} - e_{lij}E_l - h_{lij}H_l \\ D_i &= e_{ikl}\varepsilon_{kl} + \kappa_{il}E_l + \beta_{il}H_l \\ B_i &= h_{ikl}\varepsilon_{kl} + \beta_{il}E_l + \gamma_{il}H_l \end{aligned}, \tag{1}$$

- Kinematic equations

$$\varepsilon_{ij} = \frac{1}{2}(u_{i,j} + u_{j,i}), \quad E_i = -\phi_{,i}, \quad H_i = -\varphi_{,i}\,. \tag{2}$$

- Equilibrium equations

$$\sigma_{ij,i} = 0, \quad D_{i,i} = 0, \quad B_{i,i} = 0\,. \tag{3}$$

where u_i, σ_{ij} and ε_{ij} are the elastic displacement, stress, strain tensors, respectively; ϕ, D_i and E_i are the electric potential, electric displacement, electric field tensors, respectively; φ, B_i and H_i are magnetic potential, magnetic induction, magnetic field tensors, respectively; C_{ijkl}, κ_{il}, and γ_{il} are the elastic stiffness, dielectric permittivity and magnetic permeability tensors, respectively; e_{ikl}, h_{ikl} and β_{il} are the PE, PM and electro-magnetic tensors, respectively. The repetition of an index implies summation with respect to the index over its range.

2.1.2. Expanded tensor notation

By letting

$$\begin{aligned} &u_4 = \phi, \quad u_5 = \varphi, \\ &\sigma_{4j} = D_j, \quad \sigma_{5j} = B_j, \quad \sigma_{i'j'} = 0, \\ &2\varepsilon_{4j} = -E_j, \quad 2\varepsilon_{5j} = -H_j, \quad \varepsilon_{i'j'} = 0 \end{aligned}, \tag{4}$$

$$\begin{aligned} &C_{4jkl} = e_{jkl}, \quad C_{5jkl} = h_{jkl}, \\ &C_{4j4l} = -\kappa_{jl}, \quad C_{5j5l} = -\gamma_{jl}, \quad C_{4j5l} = -\beta_{jl}, \\ &C_{i'j'kl} = C_{i'j'k'l} = 0, \quad C_{i'j'k'l'} \text{ arbitrary value} \end{aligned}. \tag{5}$$

we can extend the tensors u_i, σ_{ij}, ε_{ij} and C_{ijkl} $(i,j,k,l = 1,2,3)$ respectively into u_I, σ_{IJ}, ε_{IJ} and C_{IJKL} $(I,J,K,L = 1,2,...,5)$ which meet the symmetry relations $\sigma_{IJ} = \sigma_{JI}$, $\varepsilon_{IJ} = \varepsilon_{JI}$ and $C_{IJKL} = C_{JIKL} = C_{IJLK} = C_{KLIJ}$. Here, the subscripts $i', j', k', l' = 4,5$. A Cartesian coordinate system only contains x_1-axis and x_2-axis and thus,

$$n_4 = n_5 = 0, \quad (*)_{,4} = (*)_{,5} = 0\,. \tag{6}$$

where $(*)$ denotes an arbitrary variable or expression. According to the above relations, Eqs. (1)

-(3) can be expressed in an expanded tensor notation respectively as

$$\sigma_{IJ} = C_{IJKL}\varepsilon_{KL}, \tag{7}$$

$$\varepsilon_{IJ} = \frac{1}{2}(u_{I,J} + u_{J,I}), \tag{8}$$

$$\sigma_{IJ,I} = 0. \tag{9}$$

2.2. Definition of the interaction integral

2.2.1. Interaction integral

A 2D linear MEE solid with an electrically and magnetically impermeable crack is considered. The interaction integral is the 'cross term' in the J-integral by superimposing the actual fields (u_I, σ_{IJ}, ε_{IJ}) and some known auxiliary fields (u_I^{aux}, σ_{IJ}^{aux}, ε_{IJ}^{aux}). As shown in Fig. 1, the J-integral for MEE media is [2]

$$J = \lim_{\Gamma_\varepsilon \to 0} \int_{\Gamma_\varepsilon} (F\delta_{1i} - \sigma_{ij}u_{j,1} - D_i\phi_{,1} - B_i\varphi_{,1})n_i d\Gamma. \tag{10}$$

where $F = (\sigma_{jk}\varepsilon_{jk} - D_jE_j - B_jH_j)/2$ is the electro-magnetic enthalpy density for linear MEE media, δ_{ij} is Kronecker delta and n_i is the unit outward normal vector to the contour Γ_ε. According to Section 2.1.2, the J-integral can also be expressed as

$$J = \lim_{\Gamma_\varepsilon \to 0} \int_{\Gamma_\varepsilon} (\frac{1}{2}\sigma_{JK}\varepsilon_{JK}\delta_{1I} - \sigma_{IJ}u_{J,1})n_I d\Gamma. \tag{11}$$

Superposition of an actual state and a auxiliary state leads to another equilibrium state (state S) for which the J-integral is

$$J^{(S)} = \lim_{\Gamma_\varepsilon \to 0} \int_{\Gamma_\varepsilon} [\frac{1}{2}(\sigma_{JK} + \sigma_{JK}^{aux})(\varepsilon_{JK} + \varepsilon_{JK}^{aux})\delta_{1I} - (\sigma_{IJ} + \sigma_{IJ}^{aux})(u_{J,1} + u_{J,1}^{aux})]n_I d\Gamma. \tag{12}$$

By expanding Eq. (12) as $J^{(S)} = J + J^{aux} + I$ where J and J^{aux} are respectively the J-integral corresponding to the actual state alone and the auxiliary state alone, one obtains the interaction integral as

$$I = \lim_{\Gamma_\varepsilon \to 0} \int_{\Gamma_\varepsilon} [\frac{1}{2}(\sigma_{JK}\varepsilon_{JK}^{aux} + \sigma_{JK}^{aux}\varepsilon_{JK})\delta_{1I} - (\sigma_{IJ}u_{J,1}^{aux} + \sigma_{IJ}^{aux}u_{J,1})]n_I d\Gamma. \tag{13}$$

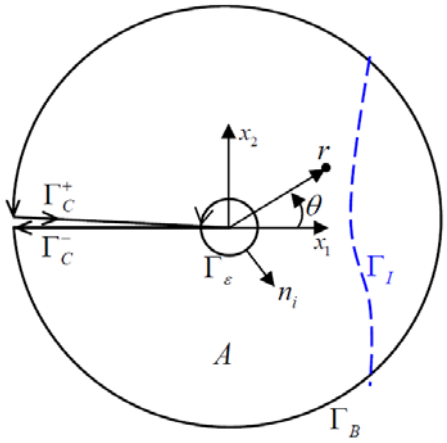

Figure 1. Integral contours around the crack tip

2.2.2. Auxiliary fields

For nonhomogeneous MEE materials, the auxiliary fields have different choices [6] and an incompatibility formulation is selected in this paper. Namely, in the polar coordinate system (r,θ) with the origin at the crack tip, the expanded auxiliary fields are defined as

$$u_J^{aux}=\sqrt{\frac{2r}{\pi}}K_N^{aux}f_J^N(\theta),\quad \sigma_{IJ}^{aux}=\frac{K_N^{aux}}{\sqrt{2\pi r}}g_{IJ}^N(\theta),\quad \varepsilon_{IJ}^{aux}=C_{IJKL}^{-1}(\mathbf{x})\sigma_{KL}^{aux} \tag{14}$$

where the index $N=\{II,\ I,\ III,\ IV,\ V\}$ denotes different crack opening modes with the value corresponding to a general subscript $I=\{1,\ 2,\ 3,\ 4,\ 5\}$; K_I^{aux}, K_{II}^{aux}, K_{III}^{aux}, K_{IV}^{aux} and K_V^{aux} denote the auxiliary mode-I, mode-II, mode-III mechanical SIFs, EDIF and MIIF, respectively. The angular functions $f_J^N(\theta)$ and $g_{IJ}^N(\theta)$ are the standard angular functions for a crack in a homogeneous MEE medium, which depend only on the material properties at the crack-tip location, and their detailed definitions can be found in Ref. [6].

2.3. Calculations of the interaction integral

The infinitesimal contour integral in Eq. (13) can not be obtained directly in numerical calculations and thus, it is usually converted into an equivalent domain integral. To begin, as shown in Fig. 1, consider a closed contour $\Gamma_0=\Gamma_B+\Gamma_\varepsilon^-+\Gamma_C^+\Gamma_C^-$ where Γ_ε^- is the opposite path of the contour Γ_ε. According to the assumption that the crack faces are assumed to be mechanical traction-free, electrically impermeable and magnetically impermeable, it can be easily proved that

$$I=-\lim_{\Gamma_\varepsilon\to 0}\int_{\Gamma_0}[\frac{1}{2}(\sigma_{JK}\varepsilon_{JK}^{aux}+\sigma_{JK}^{aux}\varepsilon_{JK})\delta_{1I}-(\sigma_{IJ}u_{J,1}^{aux}+\sigma_{IJ}^{aux}u_{J,1})]n_I q d\Gamma. \tag{15}$$

where q is an arbitrary weight function with value varying smoothly from 1 on Γ_ε to 0 on Γ_B.

When the material properties are continuously differentiable, applying divergence theorem to Eq. (15), one obtains

$$I=-\int_A\{[\frac{1}{2}(\sigma_{JK}\varepsilon_{JK}^{aux}+\sigma_{JK}^{aux}\varepsilon_{JK})\delta_{1I}-(\sigma_{IJ}u_{J,1}^{aux}+\sigma_{IJ}^{aux}u_{J,1})]q\}_{,I}dA. \tag{16}$$

where A is the domain enclosed by the contour Γ_0 for $\Gamma_\varepsilon\to 0$. According to Eqs. (7)-(9) and Eq. (14), the interaction integral in Eq. (16) can be simplified as [7]

$$I=\int_A\{(\sigma_{IJ}u_{J,1}^{aux}+\sigma_{IJ}^{aux}u_{J,1}-\sigma_{JK}^{aux}\varepsilon_{JK}\delta_{1I})q_{,I}+\sigma_{IJ,1}^{aux}[C_{IJKL}^{-1}(\mathbf{0})-C_{IJKL}^{-1}(\mathbf{x})]\sigma_{KL}q\}dA. \tag{17}$$

Compared with the expression in Ref. [6] for nonhomogeneous MEE media, the expression in Eq. (17) does not contain any term related to the derivatives of material properties with respect to the coordinates. Therefore, the present interaction integral can facilitate the facture analysis of practical MEE materials whose derivatives of material properties are difficult to obtain.

Moreover, when the integral domain A contains an interface on which the properties are discontinuous (see the dash line Γ_I in Fig. 1), A needs to be divided into two parts for using divergence theorem. Similarly to Ref. [7], the interface has no contribution to the interaction integral and thus, the same expression in Eq. (17) can be obtained. Namely, the present interaction integral does not require the material properties to be continuous, which brings a great convenience to the fracture studies of MEE composites for the integral domain can be chosen to a region containing arbitrary material interfaces.

2.4. Extraction of the fracture parameters

This section will introduce how to solve the IFs by using the interaction integral. For linear MEE

solids, the J-integral is equal to the total potential energy release rate which is expressed as [6]

$$J = \frac{1}{2} Y_{MN} K_M K_N, \quad (M, N = II, I, IV, V) \tag{18}$$

where Y_{MN} is the generalized Irwin matrix which depends on the material constants at the crack-tip location [6]. Applying Eq. (18) to the superimposed state S gives

$$J^{(S)} = \frac{1}{2} Y_{MN} (K_M + K_M^{aux})(K_N + K_N^{aux}). \tag{19}$$

By expanding Eq. (19) as $J^{(S)} = J + J^{aux} + I$, we can obtain the interaction integral as

$$I = Y_{MN} K_M K_N^{aux}. \tag{20}$$

By taking values of the vector [K_{II}^{aux}, K_I^{aux}, K_{IV}^{aux}, K_V^{aux}] to be [1, 0, 0, 0], [0, 1, 0, 0], [0, 0, 1, 0] and [0, 0, 0, 1], sequentially, Eq. (19) reduces to

$$I^{(II)} = K_{II} Y_{11} + K_I Y_{12} + K_{IV} Y_{14} + K_V Y_{15}, \tag{21}$$

$$I^{(I)} = K_{II} Y_{21} + K_I Y_{22} + K_{IV} Y_{24} + K_V Y_{25}, \tag{22}$$

$$I^{(IV)} = K_{II} Y_{41} + K_I Y_{42} + K_{IV} Y_{44} + K_V Y_{45}, \tag{23}$$

and

$$I^{(V)} = K_{II} Y_{51} + K_I Y_{52} + K_{IV} Y_{54} + K_V Y_{55}. \tag{24}$$

By simultaneously solving Eqs. (21)-(24), the IFs K_I, K_{II}, K_{IV} and K_V can be obtained.

3. Numerical implementation

3.1. Extended finite element method

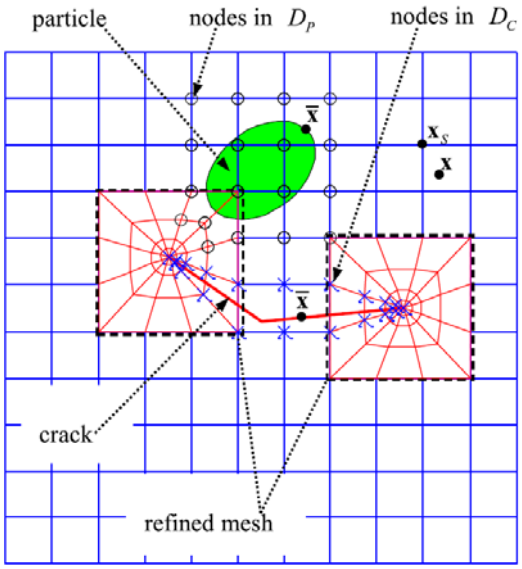

Figure 2. Finite element mesh of a plate with a crack and a particle [7]

To compute the interaction integral, the values of the actual fields u_I, σ_{IJ} and ε_{IJ} in the integral domain need to be obtained first. Generally, the numerical methods such as the finite element method (FEM), the extended finite element method (XFEM) and the element-free Galerkin method (EFGM) are adopted to compute these values. Here, the XFEM is used and the approximations of the expanded displacements are adopted as

$$u_I^h = \sum_{i\in D_S} N_{(i)} u_I^{(i)} + \sum_{i\in D_P} N_{(i)} \psi_{(i)}^b b_I^{(i)} + \sum_{i\in D_C} N_{(i)} \psi_{(i)}^c c_I^{(i)}$$
$$\psi_{(i)}^b = \left|\mathbf{x}-\overline{\mathbf{x}}\right| - \left|\mathbf{x}_{(i)}-\overline{\mathbf{x}}\right|, \quad \psi_{(i)}^c = H(\mathbf{x}-\overline{\mathbf{x}}) - H(\mathbf{x}_{(i)}-\overline{\mathbf{x}}) \tag{25}$$

where the variable marked by the index (i) denotes the value corresponding to node i; $\mathbf{x}$ is an arbitrary point; $\overline{\mathbf{x}}$ is a point on the discontinuous surface (crack or interface) which is closest to point $\mathbf{x}$; N is the standard finite element shape function; ψ^b and ψ^c are the shifted enrichment functions for material interfaces and cracks, respectively; D_S is the set of all nodes in mesh; D_P and D_C are the sets of the nodes enriched with ψ^b and ψ^c, respectively; u_I are the standard nodal displacements; b_I and c_I are additional degrees of freedom for the nodes in D_P and those in D_C, respectively; $H(\mathbf{x})$ is a Heaviside step function. In order to improve the numerical precision, the mesh around the crack tip is refined as shown in Fig. 5

In finite element computations, Eqs. (7)-(9) are usually written in the matrix form as

$$\boldsymbol{\sigma} = \mathbf{C}\boldsymbol{\varepsilon}, \quad \boldsymbol{\varepsilon} = \mathbf{L}\mathbf{u}, \quad \mathbf{L}^T\boldsymbol{\sigma} = \mathbf{0}, \tag{26}$$

where

$$\begin{aligned} \mathbf{u} &= [u_1, \quad u_2, \quad \phi, \quad \varphi]^T, \\ \boldsymbol{\sigma} &= [\sigma_{11}, \quad \sigma_{22}, \quad \sigma_{12}, \quad D_1, \quad D_2, \quad B_1, \quad B_2]^T, \\ \boldsymbol{\varepsilon} &= [\varepsilon_{11}, \quad \varepsilon_{22}, \quad 2\varepsilon_{12}, \quad -E_1, \quad -E_2, \quad -H_1, \quad -H_2]^T, \end{aligned} \tag{27}$$

$$\mathbf{L} = \begin{bmatrix} \partial/\partial x_1 & 0 & \partial/\partial x_2 & 0 & 0 & 0 & 0 \\ 0 & \partial/\partial x_2 & \partial/\partial x_1 & 0 & 0 & 0 & 0 \\ 0 & 0 & 0 & \partial/\partial x_1 & \partial/\partial x_2 & 0 & 0 \\ 0 & 0 & 0 & 0 & 0 & \partial/\partial x_1 & \partial/\partial x_2 \end{bmatrix}^T. \tag{28}$$

The material parameters in stiffness matrix $\mathbf{C}$ are given in Voigt notation. Using the relation between the indices $11\to 1$, $22\to 2$, $33\to 3$, $23\to 4$, $31\to 5$ and $12\to 6$, the constitutive Eq. (1) can be written in Voigt notation as:

$$\sigma_\alpha = C_{\alpha\beta}\varepsilon_\beta - e_{j\alpha}E_j - h_{j\alpha}H_j, \quad D_i = e_{i\beta}\varepsilon_\beta + \kappa_{ij}E_j + \beta_{ij}H_j, \quad B_i = h_{i\beta}\varepsilon_\beta + \beta_{ij}E_j + \gamma_{ij}H_j. \tag{29}$$

where the subscripts $\alpha, \beta = 1, 2, ..., 6$ and $i, j = 1, 2, 3$. For 2D MEE media, the stiffness matrix $\mathbf{C}$ in Eq. (26) is defined as

$$\mathbf{C} = \begin{cases} \mathbf{C}_{\mathrm{I}} & \text{(plane strain)} \\ \mathbf{C}_{\mathrm{I}} - \mathbf{C}_{\mathrm{II}}\mathbf{C}_{\mathrm{II}}^T/C_{33} & \text{(plane stress)} \end{cases} \tag{30}$$

where

$$\mathbf{C}_{\mathrm{I}} = \begin{bmatrix} C_{11} & C_{12} & C_{16} & e_{11} & e_{21} & h_{11} & h_{21} \\ C_{12} & C_{22} & C_{26} & e_{12} & e_{22} & h_{12} & h_{22} \\ C_{16} & C_{26} & C_{66} & e_{16} & e_{26} & h_{16} & h_{26} \\ e_{11} & e_{12} & e_{16} & -\kappa_{11} & -\kappa_{12} & -\beta_{11} & -\beta_{12} \\ e_{21} & e_{22} & e_{26} & -\kappa_{12} & -\kappa_{22} & -\beta_{12} & -\beta_{22} \\ h_{11} & h_{12} & h_{16} & -\beta_{11} & -\beta_{12} & -\gamma_{11} & -\gamma_{12} \\ h_{21} & h_{22} & h_{26} & -\beta_{12} & -\beta_{22} & -\gamma_{12} & -\gamma_{22} \end{bmatrix}, \quad \mathbf{C}_{\mathrm{II}} = \begin{bmatrix} C_{13} \\ C_{23} \\ C_{36} \\ e_{13} \\ e_{23} \\ h_{13} \\ h_{23} \end{bmatrix} \tag{31}$$

Then, Eq. (25) can be written in the matrix form as

$$\mathbf{u}^h = \sum_{i=1}^{n} N_{(i)} \left(\mathbf{u}^{(i)} + \psi_{(i)}^b \mathbf{b}^{(i)} + \psi_{(i)}^c \mathbf{c}^{(i)} \right) \tag{32}$$

where $\mathbf{b}=[b_1,\ b_2,\ b_4,\ b_5]^T$, $\mathbf{c}=[c_1,\ c_2,\ c_4,\ c_5]^T$ and n is the node number in an element.

3.2. Numerical discretization of the interaction integral

In numerical computations, the interaction integral in Eq. (17) needs to be discretized in the crack-tip local coordinate system as

$$I=\sum_{e=1}^{e_A}\sum_{p=1}^{p_e}\left\{\begin{array}{l}\left[\dfrac{\partial q}{\partial x_1}\boldsymbol{\sigma}_{\mathrm{I}}^T+\dfrac{\partial q}{\partial x_2}\boldsymbol{\sigma}_{\mathrm{II}}^T\right]\dfrac{\partial \mathbf{u}^{aux}}{\partial x_1}+\left[\dfrac{\partial q}{\partial x_1}(\boldsymbol{\sigma}_{\mathrm{I}}^{aux})^T+\dfrac{\partial q}{\partial x_2}(\boldsymbol{\sigma}_{\mathrm{II}}^{aux})^T\right]\dfrac{\partial \mathbf{u}}{\partial x_1}\\ -\dfrac{\partial q}{\partial x_1}(\boldsymbol{\sigma}^{aux})^T\boldsymbol{\varepsilon}+\dfrac{\partial(\boldsymbol{\sigma}^{aux})^T}{\partial x_1}\left[\mathbf{C}^{-1}(\mathbf{0})-\mathbf{C}^{-1}(\mathbf{x})\right]\boldsymbol{\sigma}\end{array}\right\}_p |\mathbf{J}|_p\, w_p\,. \tag{33}$$

where $\boldsymbol{\sigma}_{\mathrm{I}}=[\sigma_{11}\quad\sigma_{12}\quad D_1\quad B_1]^T$ and $\boldsymbol{\sigma}_{\mathrm{II}}=[\sigma_{12}\quad\sigma_{22}\quad D_2\quad B_2]^T$; e_A is the number of elements in the integral domain A; p_e is the number of integration points in one element; $|\mathbf{J}|_p$ and w_p represent respectively the determinant of Jacobian matrix and the corresponding weight factor at the integration point p. Here, the derivative of actual displacement vector is

$$\frac{\partial \mathbf{u}}{\partial x_1}=\sum_{i=1}^{n}\left\{\frac{\partial N_{(i)}}{\partial x_1}\mathbf{u}^{(i)}+\left(\psi_{(i)}^b\frac{\partial N_{(i)}}{\partial x_1}+N_{(i)}\frac{\partial \psi_{(i)}^b}{\partial x_1}\right)\mathbf{b}^{(i)}+\psi_{(i)}^c\frac{\partial N_{(i)}}{\partial x_1}\mathbf{c}^{(i)}\right\}. \tag{34}$$

4. Numerical examples

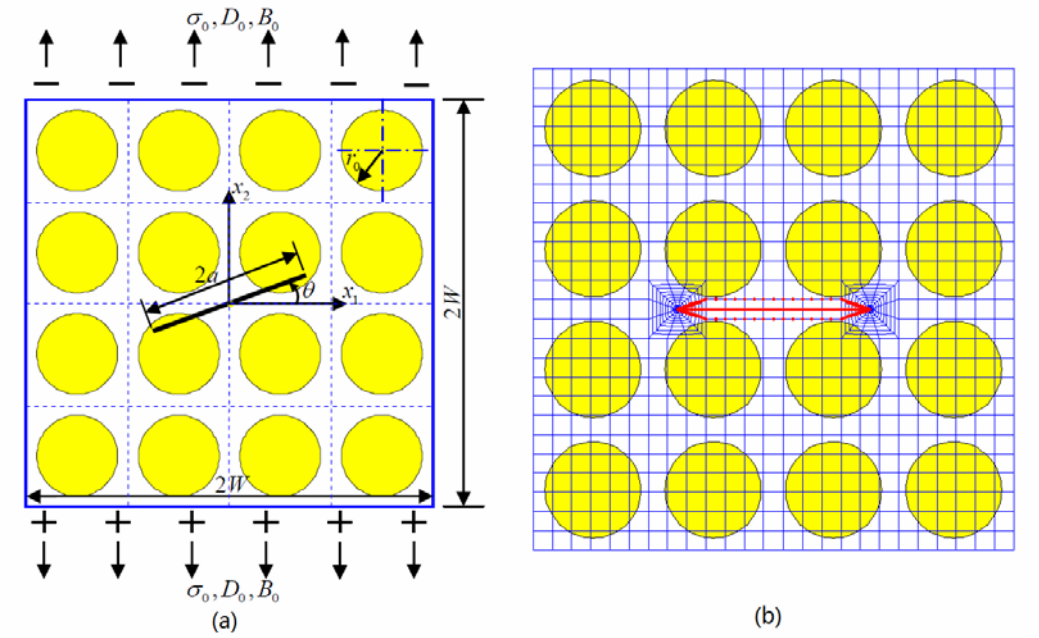

Figure 3. A 2D particulate MEE plate with a crack: (a) geometry and boundary conditions; (b) finite element mesh

As shown in Fig. 3(a), a 2D $CoFe_2O_4$ particle-reinforced $BaTiO_3$ matrix composite plate is considered. The plate of unit length ($W=0.5$) is composed of 16 square cells of length $W/2$ each of which contains a circular particle of radius r_0 at its center. Therefore, the volume fraction of the particles is $V_f=4\pi r_0^2/W^2$ and in this paper, $V_f=0.5$. In the center of the plate, there exists an inclined crack of length 2a and angle θ measured counterclockwise. The poling directions of both

the matrix and the particles are all assumed to be along x_2-axis. The magneto-electro-mechanical loading $\sigma_0 = 1$, $D_0 = 10^{-10}\sigma_0$ and $B_0 = 10^{-8}\sigma_0$ are applied along the top and bottom edges. Meanwhile, an equivalent homogeneous MEE plate of the same geometry and boundary conditions as that shown in Fig. 3(a) is adopted to compare the differences of the IFs. The material constants are given in Table 1, where the word "effective" denotes the properties of the equivalent homogeneous MEE plate.

First, we discuss a horizontal crack ($\theta = 0°$) with the crack length varying from $a/W = 0.2$ to $a/W = 0.8$. Fig. 3(b) shows the mesh configuration which consists of 1009 element and 3082 nodes. Eight-node quadrilateral (Q8) elements are used over most of the mesh and six-node quarter-point (T6qp) singular elements are employed around the crack tips. The region composed of four-layer elements around each crack tip is adopted to be the integral domain. The IFs are normalized by the factors $K_I^0 = K_{II}^0 = \sigma_0\sqrt{\pi a}$, $K_{IV}^0 = 10^{-10}\sigma_0\sqrt{\pi a}$ and $K_V^0 = 10^{-8}\sigma_0\sqrt{\pi a}$ in this paper.

Table 1. Material parameters

Parameters	C_{11}	C_{12}	C_{13}	C_{33}	C_{44}	e_{31}	e_{33}	e_{15}	
	(10^9 Pa)					(C/m^2)			
$BaTiO_3$ [8]	166	77	78	162	43	-4.4	18.6	11.6	
$CoFe_2O_4$ [8]	286	173	170.5	269.5	45.3	0	0	0	
Effective [9]	226	125	124	216	44	-2.2	9.3	5.8	
Parameters	h_{31}	h_{33}	h_{15}	κ_{11}	κ_{33}	β_{11}	β_{33}	γ_{11}	γ_{33}
	(N/Am)			(10^{-9} C^2/Nm^2)		(10^{-12} Ns/VC)		(10^{-6} Ns^2/C^2)	
$BaTiO_3$ [8]	0	0	0	11.2	12.6	0	0	5	10
$CoFe_2O_4$ [8]	580.3	699.7	550	0.08	0.093	0	0	590	157
Effective [9]	290.2	350	275	5.64	6.35	5.367	2737.5	297	83.5

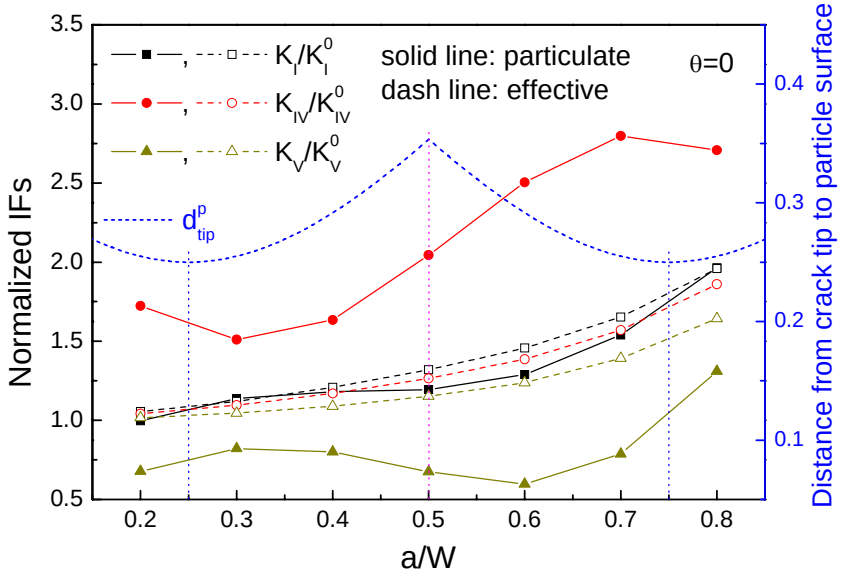

Figure 4. Normalized IFs vs crack length.

Fig. 4 shows the normalized IFs obtained at the right crack tip and the distance from the crack tip to the particle surface d_{tip}^{p}. The results show that with the increasing of crack length a/W, the

normalized IFs K_I / K_I^0, K_{IV} / K_{IV}^0 and K_V / K_V^0 are all increase monotonously for the crack in the equivalent homogeneous MEE plate while none of them varies monotonously for the crack in the particulate MEE plate. Besides, for the same geometry configuration, the EDIF (MIIF) for the particulate plate is quite larger (smaller) than that for the equivalent homogeneous plate. The reason may be that both of the crack tips are located in the PE phase.

Next, a crack of fixed length ($a/W = 0.4$) is considered and the angle θ varies from $0°$ to $90°$. As shown in Fig. 5, both of the crack tips are located in the matrix for $\theta = (0°, 90°)$ and in the particles for $\theta = 18° \sim 72°$. Fig. 6(a) and (b) show the normalized IFs obtained at the right crack tip varying with the crack angle. The results show that although obvious differences can be noted between the IFs for the particulate plate and those for the equivalent homogeneous plate, the varying trends of the SIFs are very similar for these two plates, while both the EDIF and MIIF vary distinctly with the increasing of the angle θ. The above phenomena imply that the actual PE/PM microstructures and the relative position between the crack and particles have great effects on the fracture performance of MEE composites.

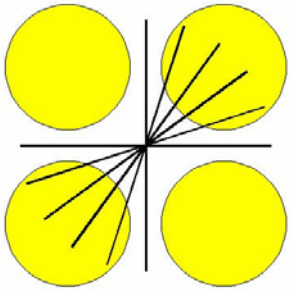

Figure 5. Crack locations for different angle θ.

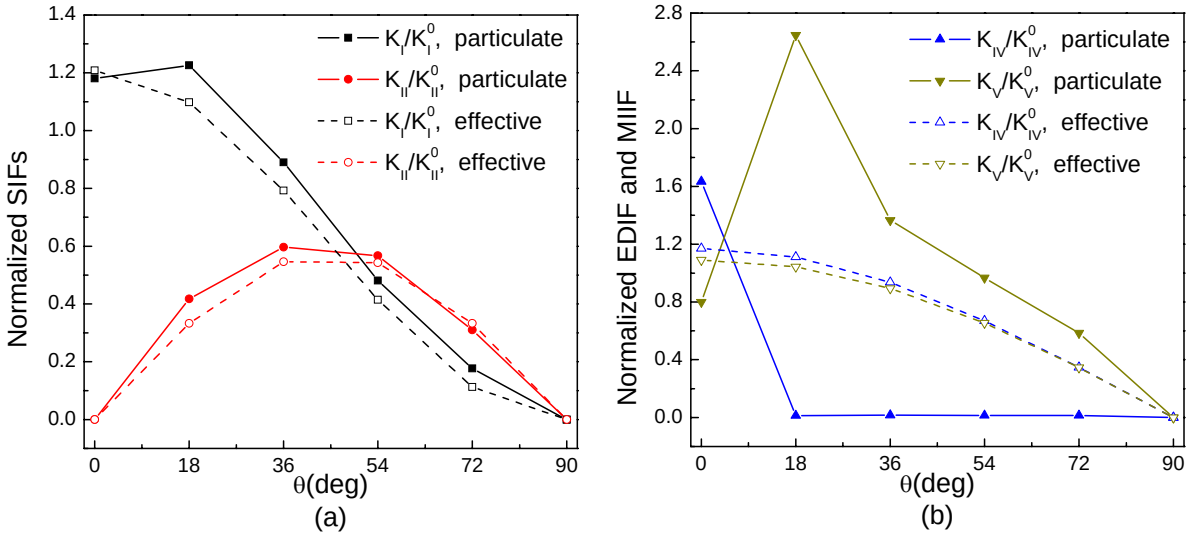

Figure 6. Normalized IFs vs angle θ for $a/W = 0.4$: (a) SIFs; (b) EDIF and MIIF.

5. Summary

MEE composites contain PE and PM phases and the interfaces between these constituent phases may reduce the reliability of MEE composites since the interfaces generally act as sources of failures in service. The complex interface environment brings a great difficulty to the fracture analysis of these MEE composites. This paper first introduces a domain form of the

interaction integral on the basis of an expanded tensor notation to solve the SIFs, EDIF and MIIF. The interaction integral does not require material properties to be differentiable and moreover, it is domain-independent for material interfaces which bring a great convenience to the fracture analysis of practical MEE composites. Using this method, the fracture problems of a particulate MEE composite are studied. The results imply that the actual microstructures of MEE composites composed of PE and PM phases have a great influence on their fracture performance.

Acknowledgements

This work is sponsored by NSFC (Grant Nos. 11072068 and 11202058), the China Postdoctoral Science Foundation (Grant Nos. 20110491071 and 2012T50338), the Fundamental Research Funds for the Central Universities (Grant No. HIT. NSRIF. 2013082).

References

[1] J.X. Liu, X.L. Liu, Y.B. Zhao, Green's functions for anisotropic magnetoelectroelastic solids with an elliptical cavity or a crack. Int J Eng Sci, 39 (2001) 1405-1418.
[2] B.L. Wang, Y.W. Mai, Crack tip field in piezoelectric/piezomagnetic media. Eur J Mech A-Solids, 22 (2003) 591-602.
[3] C.F. Gao, H. Kessler, H. Balke, Crack problems in magnetoelectroelastic solids. Part I: exact solution of a crack. Int J Eng Sci, 41 (2003) 969-981.
[4] M. Stern, E.B. Becker, R.S. Dunham, A contour integral computation of mixed-mode stress intensity factors. Int J Fract, 12 (1976) 359-368.
[5] M. Enderlein, A. Ricoeur, M. Kuna, Finite element techniques for dynamic crack analysis in piezoelectrics. Int J Fract, 134 (2005) 191-208.
[6] B.N. Rao, M. Kuna, Interaction integrals for fracture analysis of functionally graded magnetoelectroelastic materials. Int J Fract, 153 (2008) 15-37.
[7] H.J. Yu, L.Z. Wu, L.C. Guo, J.W. Ma, H. Li, A domain-independent interaction integral for fracture analysis of nonhomogeneous piezoelectric materials. Int J Solids Struct, 49 (2012) 3301-3315.
[8] L. Pasternak, Doubly periodic arrays of cracks and thin inhomogeneities in an infinite magnetoelectroelastic medium. Eng Anal Bound Elem, 36 (2012) 799-811
[9] W.J. Feng, Y.S. Li, X. Han, Z.H. Xu, Application of the extended traction boundary element-free method to the fracture of two-dimensional infinite magnetoelectroelastic solid. Sci China-Phys Mech Astron, 54 (2011) 1141-1153.